



Article

Experimental Study on the Fire-Spreading Characteristics and Heat Release Rates of Burning Vehicles Using a Large-Scale Calorimeter

Younggi Park, Jaiyoung Ryu *  and Hong Sun Ryou * 

School of Mechanical Engineering, Chung-Ang University, 84, Heukseok-ro, Dongjak-gu, Seoul 06974, Korea; pyg0511@cau.ac.kr

* Correspondence: jairyu@cau.ac.kr (J.R.); cfdmec@cau.ac.kr (H.S.R.);

Tel.: +82-2-820-5279 (J.R.); +82-2-820-5280 (H.S.R.)

Received: 8 March 2019; Accepted: 12 April 2019; Published: 17 April 2019



Abstract: In this article, large-scale experimental studies were conducted to figure out the fire characteristics, such as fire-spreading, toxic gases, and heat release rates, using large-scale calorimeter for one- and two-vehicle fires. The initial ignition position was the passenger seat, and thermocouples were attached to each compartment in the vehicles to determine the temperature distribution as a function of time. For the analysis, the time was divided into sections for the various fire-spreading periods and major changes, e.g., the fire spreading from the first vehicle to the second vehicle. The maximum temperature of 1400 °C occurred in the seats because they contained combustible materials. The maximum heat release rates were 3.5 MW and 6 MW for one and two vehicles, respectively. Since the time to reach 1 MW was about 240 s (4 min) before and after, the beginning of the car fire appears to be a medium-fast growth type. It shows the effect on the human body depending on the concentration of toxic substances such as carbon monoxide or carbon dioxide.

Keywords: fire-spreading characteristics; real vehicle experiments; toxic gases; temperature distributions; unsteady heat release rate

1. Introduction

Many vehicle fire studies are being carried out since vehicle accidents result in catastrophe due to various reasons such as drivers' negligence, electrical faults, deliberately lit and arson in parking lots [1], buildings, and tunnels, and so forth. To prevent vehicle disasters and suggest a guideline for evacuees in case of emergency, figuring out the fire-spreading mechanism and measuring other key parameters such as heat release rates and temperatures are necessary to install sprinklers, smoke control systems, and setting up fire extinguishers.

In fire researches, calorimeters, which can estimate a heat release rate, smoke generation, carbon dioxide, carbon monoxide, and so on, have been widely used for experimental study [2–5]. In the case of heat release rate, it has been regarded as one of the most important factors during experimental studies since it can be used to calculate the size of the fire and be more easily used in performance-based design (PBD). Large-scale tests are considered the most accurate way to secure fire-spreading effect and heat release rate, however, there is limited research, as it cost too much [6–8]. Katsuhiro et al. [6] found that the temperature distribution and maximum HRR reached 3 MW by changing the initial ignition location of the fire. In addition, they found that the fire spread radically after the windows were broken. Throughout related large-scale experiments, a single vehicle represents the heat release rate of 2.5–5 MW. However, most of the experimental studies were conducted only on one vehicle. Vehicle fires normally occur between two vehicles because of accidents. Li et al. [9] conducted large-scale experiments using

two sedan vehicles to determine the change of the temperature distribution; however, in this study, the heat release rate was not considered, although it is an imperative part not only for analyzing the fire phenomena, but also suggesting guidelines for rescue as a function of time. Therefore, we investigated fire-spreading phenomena considering the effect of two vehicles fire scenario to figure out an important parameter such as heat release rates, fire-spreading time, and so forth.

A secondary factor that causes catastrophe in vehicle fires is the influence of toxic gases, e.g., carbon monoxide (CO) and carbon dioxide (CO₂), on human breathing and other functions [10–12]. Truchot et al. [13] investigated toxic-gas emissions from vehicle fires in tunnels. They did experimental studies using large-scale facilities, where the air flow in the tunnel could be controlled. They found and measured the toxic substances through a flame ionization detector/analyzer. It showed the toxic substances emitted in the tunnel shaft and analyzed the effects of various heat release rates. Smoke and toxic gases that are produced in the open are released into the air, due to their buoyancy. However, when a vehicle burns in an enclosed space, e.g., a tunnel or an indoor parking lot, the gas cannot escape to the atmosphere. Therefore, it is one of the main factors that should be considered in fire research to understand the concentration of the toxic substances generated when a vehicle fire occurs. However, there is limited information regarding the toxic gases that appear in the event of the fire.

Furthermore, many experimental studies are being actively carried out with pool-fire tests to represent fire accidents in tunnels or high-rise buildings [14–23]. Beak et al. [23] conducted tunnel-fire experiments using small-scale tunnels with pool fires, because it is challenging to experiment in real tunnels with real vehicles. He provided detailed information on the fire's heat release rate and its hole-plugging effect on tunnels; however, the results were obtained from pool-fire experiments, not real vehicles. It is clear that the results obtained from real products and pool-fire experiments will be different.

Therefore, it is necessary to analyze the fire-spreading characteristics of an actual vehicle and analyze the heat release rate and temperature distribution in order to understand the fire phenomena and its applications. Figure 1 represents a schematic diagram of the basic concept for this study. In this study, the fire-spreading characteristics, unsteady heat release rate, and the toxic substances in vehicle fires are measured using a large-scale calorimeter. All information, such as the change of heat release rate, temperature distributions and toxic gases as a function of time, gained throughout this research can be applied to other fire-related researches regarding vehicles and tunnels, parking lots, and so forth.

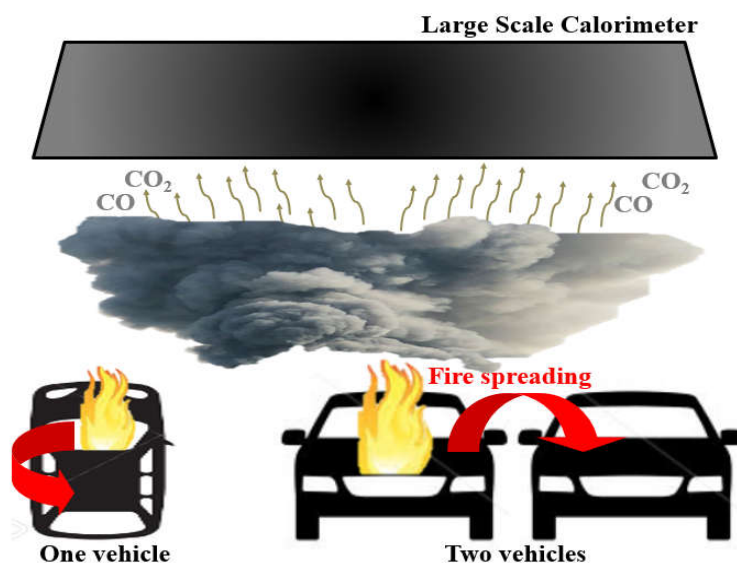


Figure 1. Schematic diagram of the basic concept for this study.

2. Experimental Setup and Conditions

Experiments were conducted using a large-scale calorimeter (LSC) from the Korea Institute of Construction Technology (KICT), applicable up to 10 MW, to determine the unsteady heat release rate and toxic gases, e.g., CO and CO₂, generated by the fire. The schematic diagram of LSC is represented in Figure 2 to figure out the values regarding change of the heat release rate and toxic substances as a function of time, and specifications of the experimental apparatus are represented in Table 1.

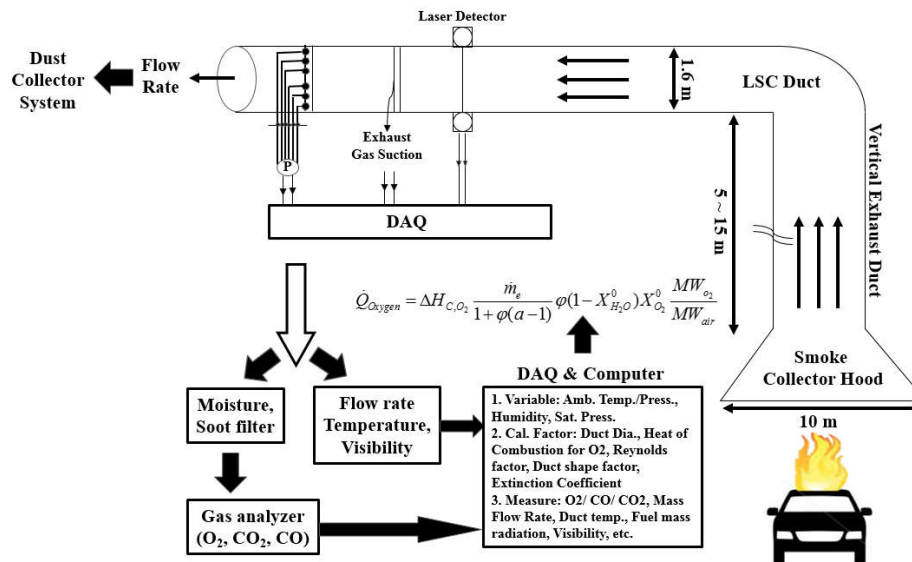


Figure 2. Schematic diagram of large-scale calorimeter (LSC) used to detect the changes in the heat release rate and toxic substances as a function of time.

Table 1. Specification of experimental apparatus.

Measurement	Specification
Duct pressure difference	Output: 4–20 mA, Range: 0–1245 Pa Model: PADT-D1000 Pa
Duct Temperature	K-type wire, Range: –200–1000 °C
Gas Analyzer	Output: 4–20 mA, Range: O ₂ 20.95%, CO ₂ 8%, CO 0.8% Model: Servomax 4100
Laser	Output: 0–8.4 mV, Range: 0–100% Model: 25-LHP-213-249
Load Cell	Output: 4–20 mA, Range: 0–3000 kg Manufacturer: Sartorius
Heat Flux	Plate Type, Range: –200–1000 °C Model: GTW-10-32-485A
Mass Flow	Output: 4–20 mA, Range: 0–2500 L/min Model: DPE-S

To investigate the fire-spreading characteristics and temperature distributions for one and two vehicles, K-type thermocouples (OMEGA, measuring range: –200–1260 °C) were attached to the engine room, bumpers, seats, and fuel tank. Temperature data were transmitted to a data-acquisition unit (DAQ) on a PC every second, and the experiments were recorded by a video recorder. The initial ignition location was assumed to be the passenger seat. Figure 3 represents the experimental setup and conditions. In the two-vehicle experiment, the distance between vehicles was set to 50 cm, and the thermocouples were attached in the same positions. The fuel was almost eliminated to prevent explosions during the experimental study.

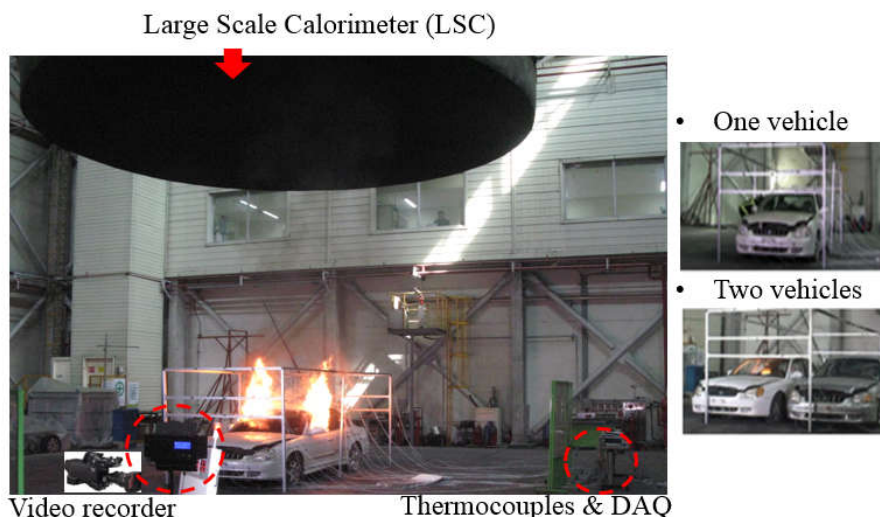


Figure 3. Experimental setup and measurement tools.

Four-door sedan vehicles were used in the experiments. The vehicle size was 4.7 m (length) × 1.8 m (width) × 1.4 m (height), and was Hyundai’s EF sonata released in 1998. These vehicles have not been used for about 10 years, and the experiment was carried out after the pressure of tires were removed with opening full front windows. The location and number of thermocouples in each compartment are represented in Figure 4. Thermocouples were attached to the engine room, bumpers, seats, and fuel tank. Sixteen thermocouples were attached to the engine room, four each at the top and bottom, and two on each side. Ten thermocouples were attached to the bumpers; five each on the front and rear. In addition, 14 thermocouples were attached to each seat in the vehicle interior, representing the head, waist, legs, and feet. Twelve thermocouples were attached to the fuel tank, one on each side, and four each on the top and bottom. Thus, 42 thermocouples were used to figure out the change of the temperature distribution as a function of time.

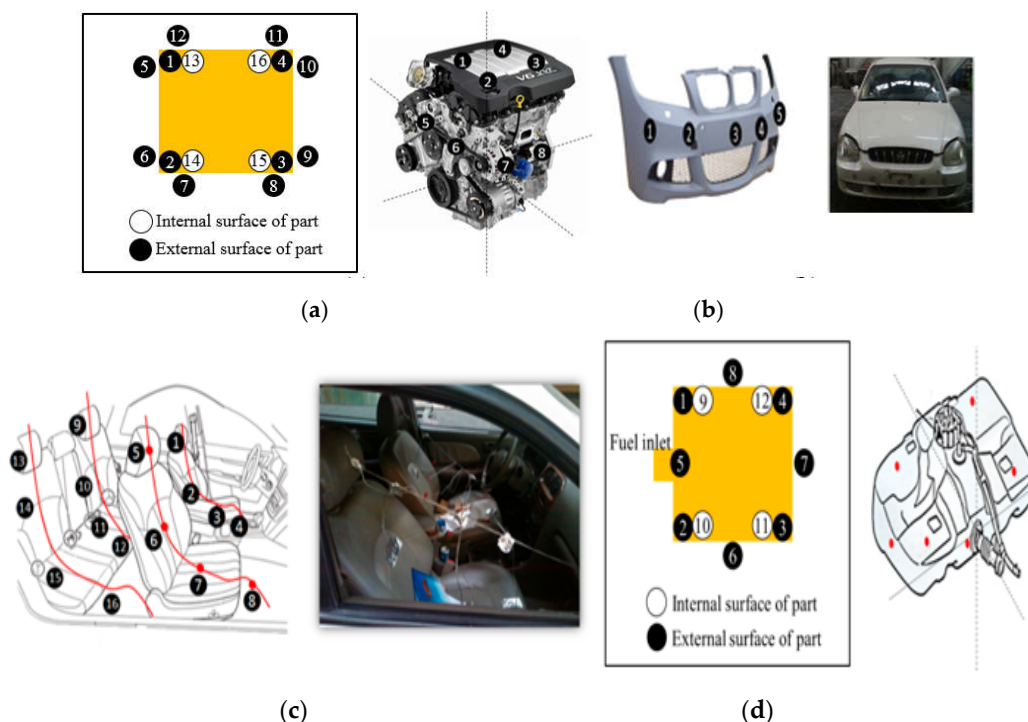


Figure 4. Location and number of thermocouples: (a) Engine room, (b) bumpers, (c) vehicle interior, and (d) fuel tank.

3. Results and Discussion

3.1. Fire-Spreading Characteristics

Fire-spreading over one and two vehicles as a function of time while on experiments are presented in Figure 5. Also, a flow-chart about fire-spreading inside a vehicle and two vehicles as a function of time are represented in Figure 6. These represent the major fire-spreading points as a function of time. As represented in the Figure 5 and the flow-chart, in the one-vehicle experiments, the fire spread to the driver seat and rear seat almost simultaneously, followed by the fuel tank, engine room, and finally the front and back bumpers. In the two-vehicle experiments, the fire followed the same sequence until it spread to the next vehicle, due to radiation. It then spread simultaneously to the rear seat and driver seat of the second vehicle, then the engine room, fuel tank, and bumpers in a regular sequence. Detailed information on the fire-spreading characteristics and special events as a function of time are represented in Table 2.

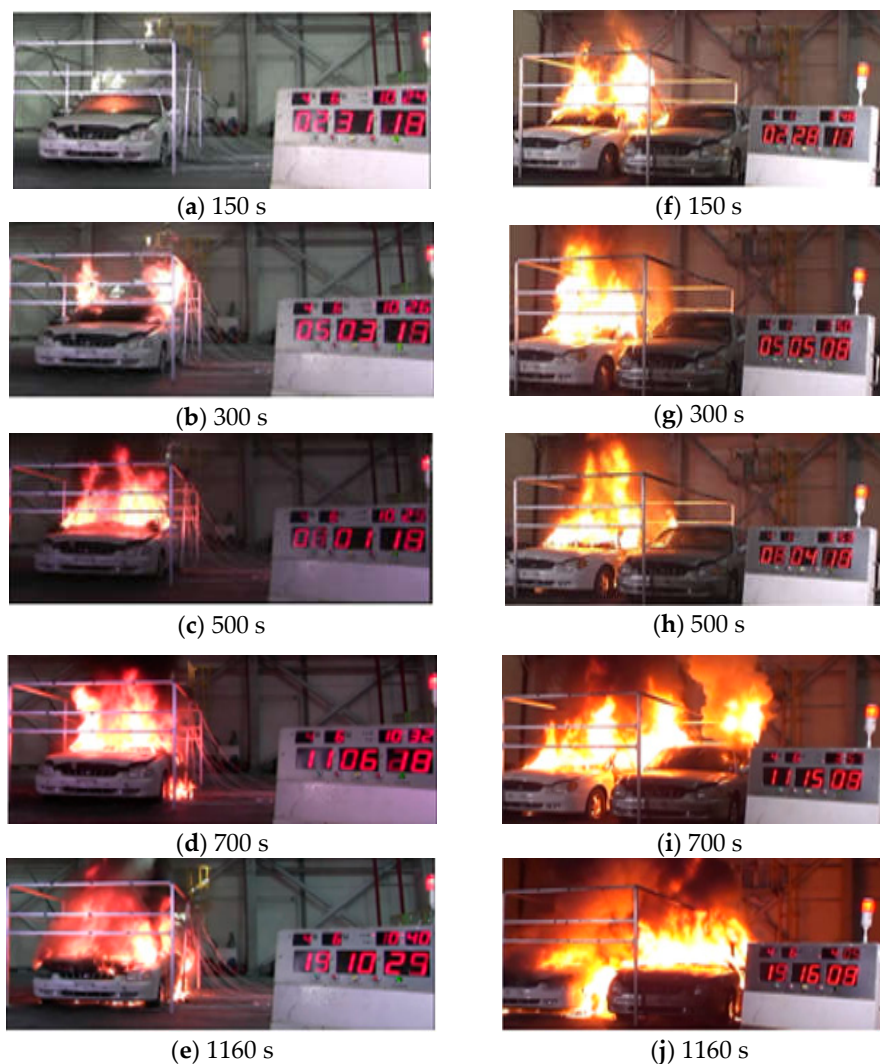


Figure 5. Fire spreading as a function of time for one and two vehicles; (a) 150 s after fires in one vehicle, (b) 300 s after fires in one vehicle, (c) 500 s after fires in one vehicle, (d) 700 s after fires in one vehicle, (e) 1160 s after fires in one vehicle, (f) 150 s after fires in two vehicles, (g) 300 s after fires in two vehicles, (h) 500 s after fires in two vehicles, (i) 700 s after fires in two vehicles, and (j) 1160 s after fires in two vehicles.

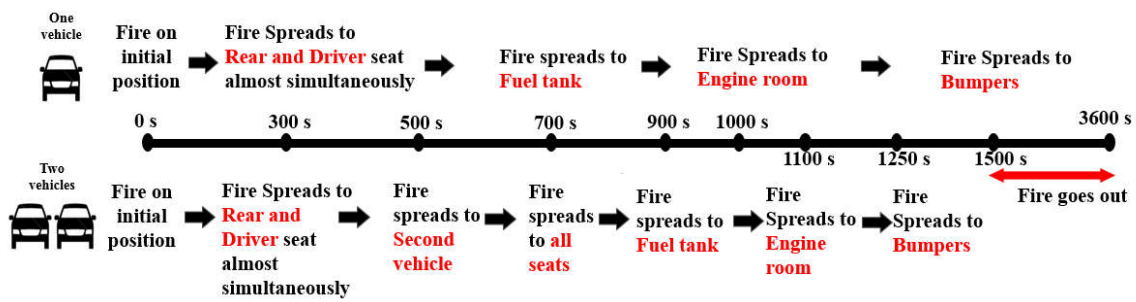


Figure 6. Major fire-spreading flow-chart.

Table 2. Detailed information on the fire-spreading characteristics and special events as a function of time.

Time (s) After Ignition	Fire Reaches Maximum Temperature and Goes Out	
	First Vehicle	Second Vehicle
0	Ignition in passenger seat	
150	Fires active in passenger seat	
300	Fire spreads to driver and rear seats almost simultaneously	
500	-	Fire spreads to the second vehicle
700	Fire spreads to fuel tank	Fire dramatically spreads to seats
900	-	Fire spreads to fuel tank
1000	Fire spreads to engine room	-
1100	-	Fire spreads to engine room
1250	-	Fire spreads to bumpers
1500	Fire spreads to bumpers	-
1500–3600	Fire goes out	Fire goes out

Therefore, the main temperature changes in the seats, engine room, fuel tank, and bumpers were represented. The temperature distribution on seats are represented in Figure 7. The passenger seat actively caught fire around 300 s (5 min) after ignition, and the highest temperature was observed in the interior, due to its combustible materials compared with the other compartments.

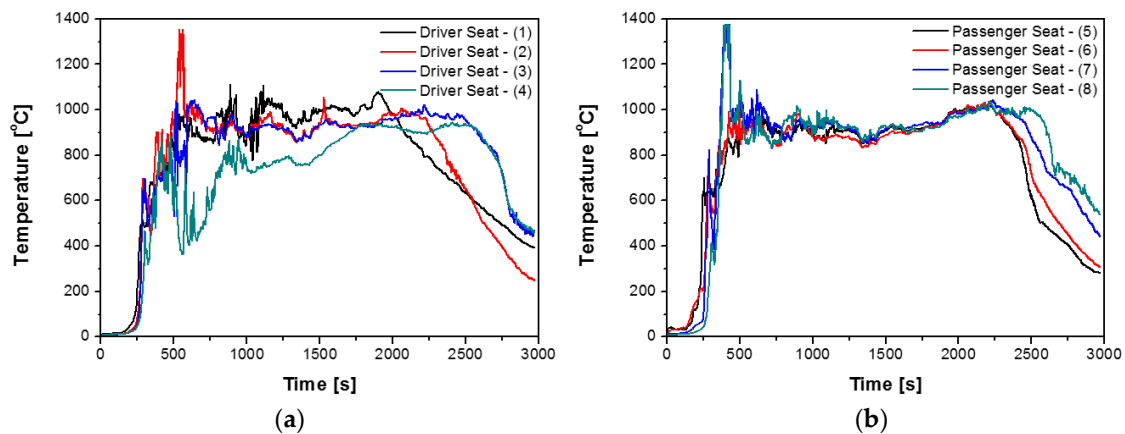


Figure 7. Temperature distribution on seats of the first vehicle; (a) temperature of driver seat in first vehicle and (b) temperature of passenger seat in first vehicle.

The fire spread to the driver and rear seats simultaneously; however, the temperature differed slightly, as can be seen in Figure 8, which represents the temperature distribution of the driver and rear seats for the two sets of vehicles. The temperature increase in the driver seat and the rear seat can be observed almost simultaneously. The beginning of the temperature increase and the highest temperature are represented as the green and red lines, respectively. This means that the fire in the driver seat was larger than the rear seat, even though the fire-spreading time was similar because the driver seat was located closer to the fire than the rear seat.

To investigate the effect of temperature propagation on the number of vehicles, the driver seat and the rear seat inside the first vehicle are represented in Figure 8a,b. In the case of Figure 8c,d, it showed the driver seat and the rear seat inside the first vehicle when the two-vehicle experiment. After 500 s (8 min 20 s), the fire spread to the next vehicle, and the interior's temperature rapidly increased around 700 s (11 min 40 s), as shown in Figure 8c,d. Since the second passenger seat was located next to the first vehicle, the fire reached the thermocouple's temperature limit of 1370 °C.

The analysis was begun by dividing the time into sections for the various fire-spreading periods and major changes. Section 1 represented the period of the fire spreading from the passenger seat to the driver and rear seats after 300 s (5 min). Section 2 was 500 s (8 min 20 s) after the ignition, in which the fire spread to the next vehicle. Section 3 was when both the passenger seat and driver seat of the second vehicle caught fire. Section 4 was the period when the HRR reached maximum in the case of two-vehicle fire. These same sections were used for representing the heat release rates and the toxic substances in Sections 3.2 and 3.3, respectively.

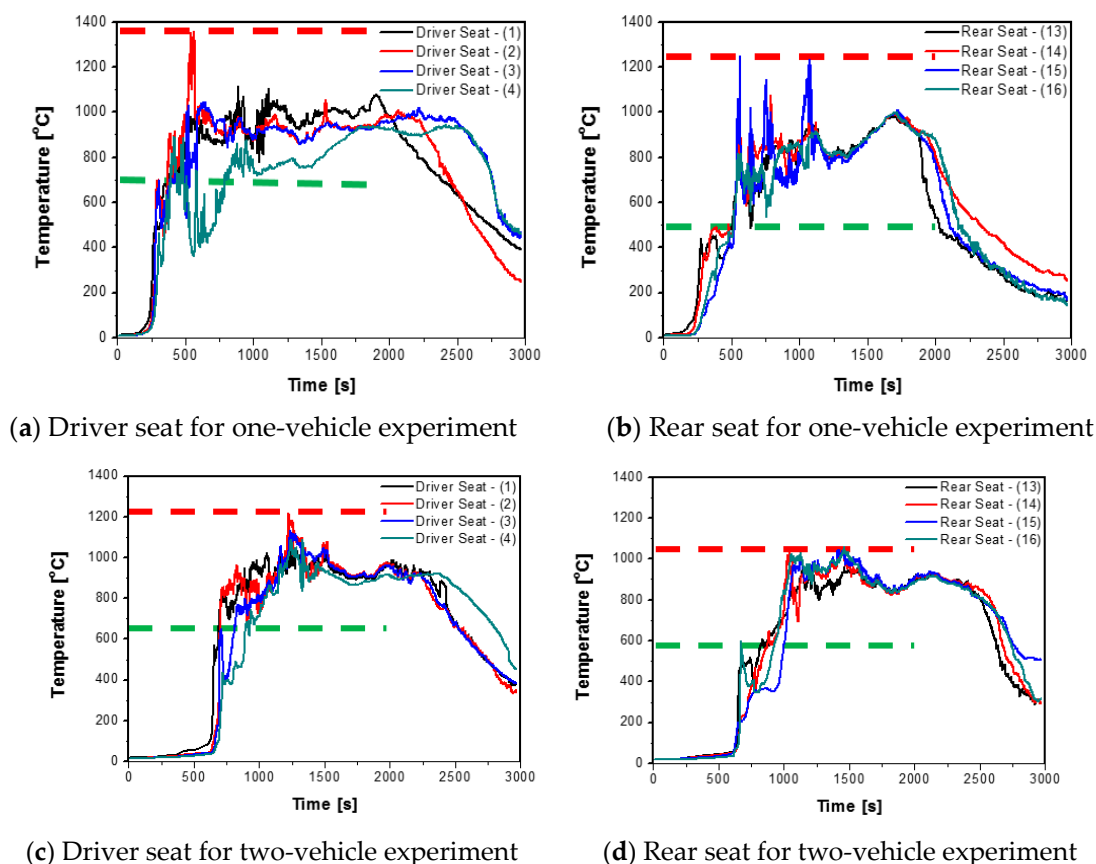


Figure 8. Temperature distribution results inside the driver and rear seats for one and two vehicles: (a) Temperature of driver seat inside the first vehicle for the one-vehicle experiment, (b) temperature of rear seat inside the first vehicle for the one-vehicle experiment, (c) temperature of driver seat inside the first vehicle for the two-vehicle experiment, and (d) temperature of rear seat inside the first vehicle for the two-vehicle experiment.

The temperature distribution in engine room and fuel tank were represented in Figure 9. The engine room was comprehensively burning within about 1200 s (20 min) of the fire ignition. In addition, the fire in the initial vehicle did not propagate directly to the engine room, but first spread to the seats. After about 1300 s (21 min 40 s), the fire spread to the adjacent vehicle. The fire went out 2500 s (41 min 20 s) after reaching the maximum temperature.

In the fuel tank, the temperature change was relatively small compared to the other combustibles. This was because most of the fuel was removed; however, in a real vehicle fire, it is the most vulnerable and dangerous compartment for the fire to reach.

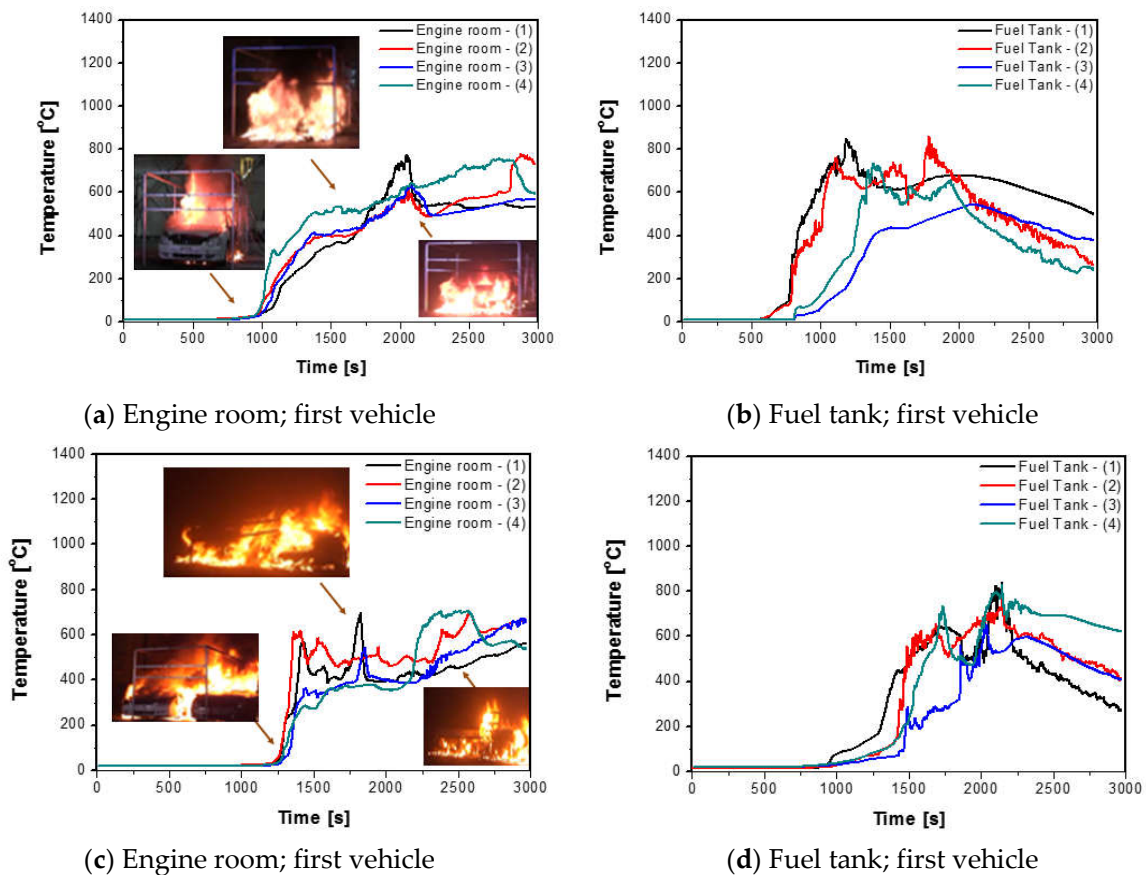


Figure 9. Temperature distribution in the engine room and fuel tank for one and two vehicles: (a) Temperature of engine room in first vehicle in the one-vehicle experiment, (b) temperature of fuel tank in first vehicle in the one-vehicle experiment, (c) temperature of engine room in first vehicle in the two-vehicle experiment, and (d) temperature of fuel tank in first vehicle in the two-vehicle experiment.

The temperature distributions at the bumpers are represented in Figure 10. For the front bumper, the temperature rose from the place nearest the initial fire vehicle. After about 1400 s (23 min 30 s), the temperature rose in the next vehicle. The temperature rose later because it was located farthest from the first vehicle. In addition, in the rear bumper, the fire spread more quickly than the front bumper because it was relatively close to the seat.

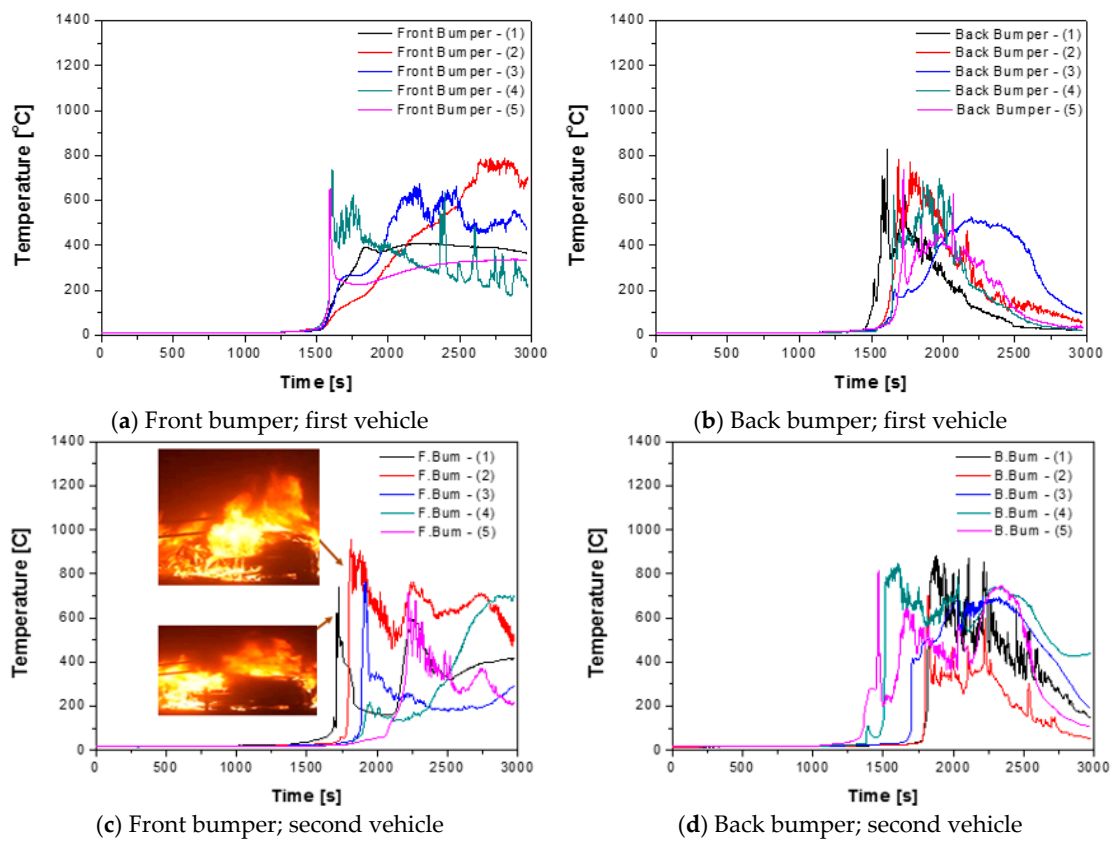


Figure 10. Temperature distribution at bumpers for one and two vehicles: (a) Temperature of front bumper in first vehicle, (b) temperature of back bumper in first vehicle, (c) temperature of front bumper in second vehicle, and (d) temperature of back bumper in second vehicle.

3.2. Heat Release Rate

The heat release rates considering the unsteady fire phenomenon are represented in Figure 11. As can be seen in Figure 6, the heat release rate increased rapidly around 180 s (3 min) after ignition because the fire spread into the vehicle interior. Further, when the windshield broke around 300 s (5 min), the heat release rate increased sharply to about 2.3 MW. However, it continued to increase because the fire spread from the passenger seat to the driver seat. The passenger-seat cushion spontaneously ignited and then temporarily decreased. Because the cushion was composed of a composite material, the heat release rate increased and decreased repeatedly until it reached its maximum.

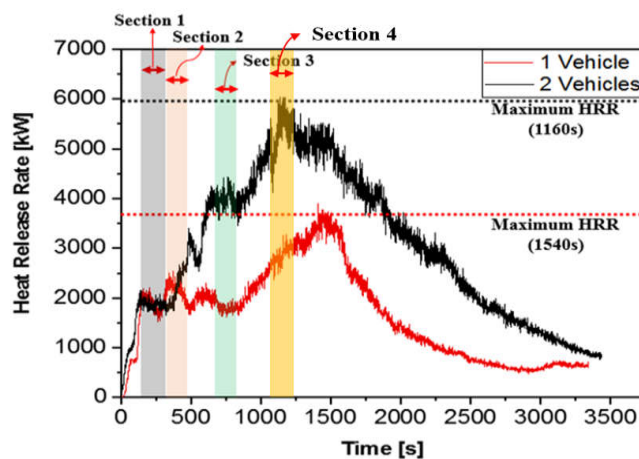


Figure 11. Heat release rate for one and two vehicles as a function of time.

For the engine room and the fuel tank, the increasing and decreasing heat release rate was not apparent because there was little fuel in the engine room and the engine oil was low. After reaching the maximum heat release rate of 3.5 MW, the fire slowly went out.

In the case of the two-vehicle experiments, the heat release rate followed a similar pattern until the initial window breakage. After that, the fire spread to the entire passenger seat and then the next vehicle at about 600 s (10 min), due to radiation. After the ignition, the fire spread rapidly through the open passenger window. The spacing between the vehicles was about 50 cm, and there was a 2 MW fire around the vehicle. When both vehicles were burning, the fire spread dramatically to all of the seats. The maximum heat release rate was about 6 MW, and the fire went out gradually. Since the time to reach 1 MW was about 240 s (4 min), the fire growth in a vehicle is considered to be a medium-fast fire.

The heat release rate is one of the most important parameters to calculate the flame height [24,25]. McCaffrey [24] presented several formulas under various conditions, but, one of the functions under the open condition can be calculated the flame height using heat release rate. McCaffrey's formula is as follows:

$$Z_c = 0.08 Q^{2/5} \quad (1)$$

where Z_c (m), Q (kW) are flame height and the heat release rates, respectively. Throughout this formula, the maximum flame heights were calculated as 2.1 m and 2.6 m for one and two vehicles, respectively.

Furthermore, the height of the flame in normal atmospheric conditions was indicated by non-dimensional analysis [25], and it is as follows:

$$L_f = 0.235 \cdot Q^{2/5} - 1.02D \quad (2)$$

where L_f (m), Q (kW), D (m) are flame height, the heat release rates, and diameter of pool, respectively. In case of the function suggested by Heskestad [25], the flame height can be calculated using the heat release rate and pool diameter. Throughout this formula, the maximum flame heights were calculated 4.3 m and 7.6 m, 1.35 m and 2.83 m, and 3.49 m and 4.97 m for one and two vehicles for varying diameters, respectively. Because the width and length of the vehicle have different diameters, the flame heights were calculated with the diameters at 1.8 m width, 4.7 m length, and 2.6 m hydraulic diameter of the vehicle. Flame heights are represented as a function of time and maximum flame heights in Figure 12 and Table 3, respectively. However, measuring the change of flame heights was affected significantly under various conditions.

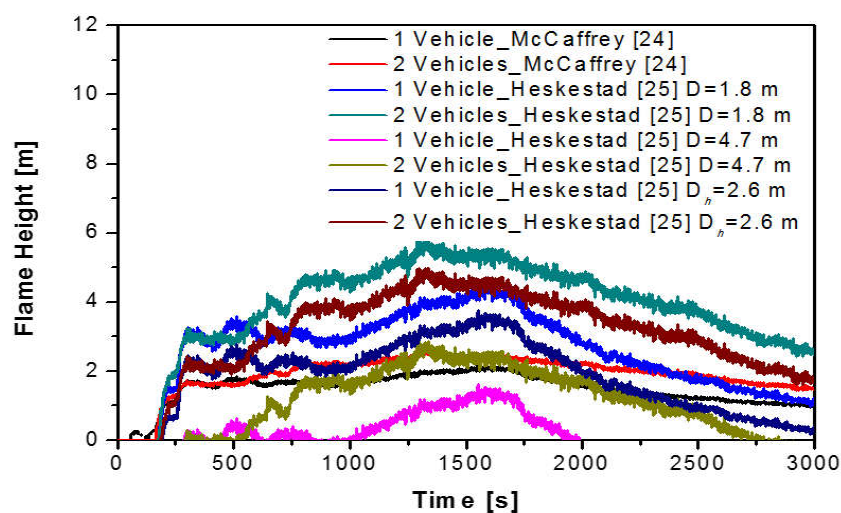


Figure 12. Flame height calculated by Equation 1 (McCaffrey [24]) and Equation 2 (Heskestad [25]) for varying diameter as a function of time.

Table 3. Comparison of flame heights under the open condition.

Number of Vehicle	Maximum Flame Height (m)			
	McCaffrey [24]		Heskestad [25]	
	-	$D = 1.8$	$D = 4.7$	$D_h = 2.6$
One	2.1	4.3	1.35	3.49
Two	2.6	7.6	2.83	4.97

The fire growth can be evaluated using the following generic fire-growth curve:

$$Q_{\max} = a \cdot (t - t_i)^2 \quad (3)$$

where a is the fire-growth coefficient (kW/s^2), t means time (s), and t_i means the time of ignition (s). In this study, the time of ignition can be taken as zero. The fire-growth coefficients for vehicle fires up to 1 MW are represented in the Appendix A. Reducing the flame height and fire growth were decisive parameters for suppressing a fire; a fire extinguisher should be considered, especially in enclosed spaces, e.g., tunnels and indoor parking lots.

It is generally well acknowledged that fire experiments are really difficult to do repeated experiments, due to time consumption and expensive time. Thus, various fire articles did not contain a detailed uncertainty analysis. Melcher et al. [26] suggested the impact of random deviations that may occur in a single experiment. Mass loss rates and heat release rates for one and two vehicles were represented with error range in Figure 13. Yellow and lavender indicate the error ranges that occurred in one and two vehicles, respectively.

Applying the actual heat release rates obtained from this study to the numerical analysis study, Park et al. published a study on the effect of a vehicle accident on the evacuation in various tunnel aspect ratio [27].

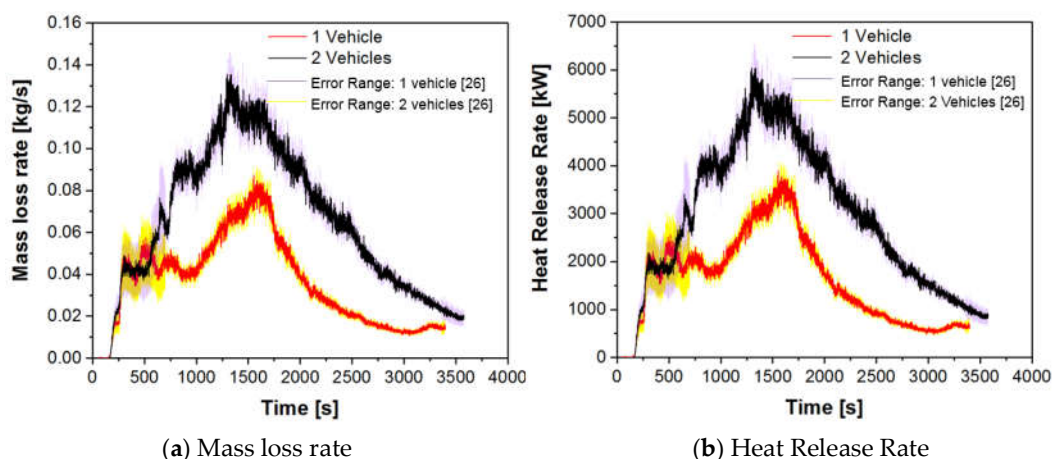


Figure 13. Mass loss rate and heat release rate for one and two vehicles as a function of time, error range estimated following Melcher et al. [26]: (a) Mass loss rate and (b) heat release rate.

The maximum heat release values obtained by other studies are shown in Table 4 and compared with the results obtained through this experiment. As a rule of thumb, the maximum heat release rates were normally represented 2.5 MW to 5 MW. Okamoto et al. [8] found the heat release rates as a function of time in real-scale experiments, and the vehicles used in this experiment were similar to those used in this study. The experimental conditions were quite similar, such as conducting the vehicle fire test in the absence of fuel, but only with different experimental measuring equipment. In addition, the maximum heat release rate was 3.5 MW, the same as this study. However, in the case of research done by Shipp et al. [28], the maximum heat release rate was significantly higher than other studies

since the vehicle tests involved fuel spill from the petrol tank. Furthermore, Ingason [29] conducted the vehicle fire experiments in a tunnel so that the maximum heat release rates were different because of ceiling temperatures, ventilation system on maximum heat release rate, and fire growth rates.

Table 4. Comparison of maximum heat release rates throughout large-scale experiments.

Type of Vehicles	Maximum Heat Release Rate (MW)			
	Okamoto et al. [6]	Shipp et al. [28]	Ingason [29]	Park et al.
Small passenger car	3.5	8	2.5	3.5
Large passenger car	4.2	-	<5	-
2 passenger cars	-	-	3.5–10	6

3.3. Toxic Substances

The changes in the amounts of carbon dioxide and carbon monoxide as a function of time are represented in Figure 14. These values represent the toxic gases obtained through the LSC from the vehicle as it burned. The main changes on carbon monoxide and carbon dioxide as a function of time are represented in Tables 5 and 6, respectively. Furthermore, it showed similar trends to the distribution of change of heat release rate. However, judging from the influence on the human body, it is obvious that these values might be not correct, because of the many differing conditions in fire phenomena, e.g., enclosed or open spaces, scale of space, ventilation systems, sprinklers, and so on.

With fires in open spaces, the smoke and toxic gases will be released into the air. In enclosed spaces, e.g., tunnels or indoor parking lots, the smoke will accumulate continuously, and the concentration will greatly increase. However, the effects on the human body can be analyzed based on concentrations of CO and CO₂ from the vehicle itself [30].

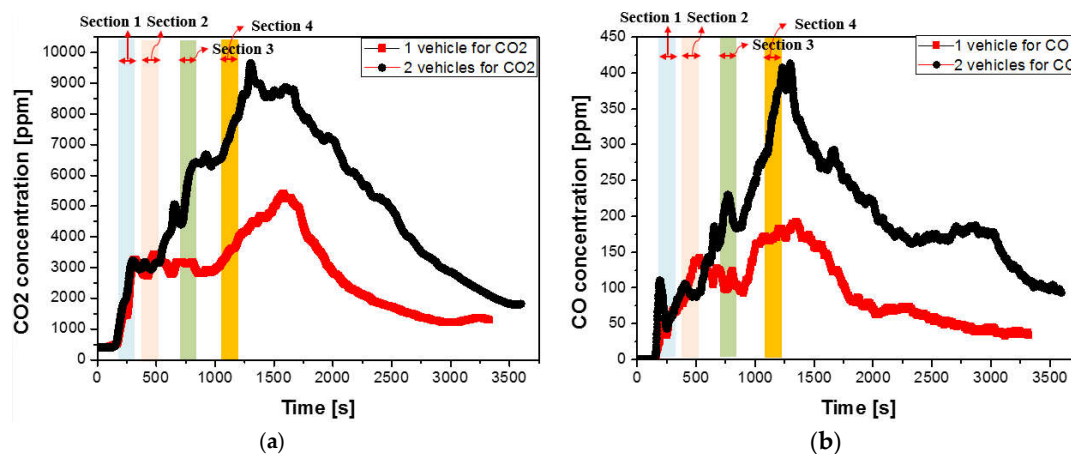


Figure 14. Toxic-substance concentration results: (a) Carbon dioxide and (b) carbon monoxide.

Table 5. Carbon-dioxide concentration at the major change periods, and influences on the body based on value.

Section	CO ₂ Concentration (ppm)		Effect on Health [30]	
	One Car	Two Cars	One Car	Two Cars
Section 1	1000–3000		General condition and mild headaches	
Section 2		3000	Poor air condition and headaches	
Section 3	3000	4500–6200	Poor air condition and headaches	
Section 4	3000–3500	6500–8000	Headaches	Respiratory, circulatory, and cerebral impairment

Table 6. Carbon-monoxide concentration at the major change periods, and influences on the body based on value.

Section	CO Concentration (ppm)		Effect on Health [30]	
	One Car	Two Cars	One Car	Two Cars
Section 1	0–50	0–100		Slight headaches
Section 2		75–150		Headaches
Section 3	100–125	150–225	Headaches	Dizziness, nausea, fatigue, headaches
Section 4	150–175	300–425	Dizziness, nausea, fatigue, headaches	Headache and nausea; life threatening in 3 h

Based on the values obtained from the LSC, the CO₂ generated from one vehicle will give a person a slight headache. However, in a two-vehicle fire, the slight influence occurs before 1000 s (16 min 40 s); however, after that, it will affect the respiratory system and nervous system, and cause cerebral impairment. Furthermore, only a slight headache can be felt about 500 s (8 min 20 s) after ignition. However, after that, the area should be evacuated. In the worst case, life is threatened, and evacuation may be difficult because of the high concentration of CO over 1200 s (20 min). The higher the heat release rate is, the higher the concentration of CO and CO₂. Therefore, the larger the fire is, the faster the area should be evacuated. Based on the CO and CO₂ concentrations absorbed through the LSC, the impact on human health applies when people were directly exposed. It is apparent that the values obtained through the LSC will vary depending on the location and conditions of the fire inside of buildings, but it can provide indirect guidance on ventilation and evacuation in compartment space while presenting the toxic concentration occurring in the vehicle itself.

4. Conclusions

The aim of this study was to investigate how fire spreads through a vehicle using an actual vehicle-fire test, and to analyze the heat release rate for two vehicles using a large-scale calorimeter. In addition, the influence of the toxic gases generated from the vehicle fires was analyzed. An analysis of the experimental results provided the following conclusions.

- (1) In actual vehicle tests, the fire spread from the initial ignition location to the rear seat, engine room, fuel tank, and bumper in regular sequence. In the two-vehicle situation, a similar tendency was observed, and the fire spread to the next vehicle after about 500 s (8 min 20 s).
- (2) The fire rose sharply after 200 s (3 min). The maximum heat release rates of one and two vehicles were represented as 3.5 MW and 6 MW, reached at about 1540 s (25 min 40 s) and 1160 s (19 min 20 s), respectively. Since the time to reach 1 MW was about 240 s (4 min) before and after, the fire growth in a vehicle fire is considered to be a medium-fast fire phenomenon.
- (3) The evacuation should be totally completed within 20 min after the fire starts, because of the high concentrations of carbon dioxide and carbon monoxide in an enclosed space. This may vary, depending on the size of the location where the fire occurs.
- (4) In this study, uncertainty analysis cannot be included because of financial problems like other related studies [6–8], however, we place emphasis on fire-spreading characteristics inside of a vehicle and toxic gases.

Author Contributions: Conceptualization, methodology, investigation, formal analysis, Y.P. and J.R.; writing—original draft preparation, Y.P.; writing—review and editing, J.R.; project administration, supervision, H.S.R.

Funding: This research was supported by the Research and Development to Enhance Firefighting Response Ability founded by National Fire Agency (2018-NFA002-007-01010002-2018) and Chung-Ang University Research Grants in 2017.

Conflicts of Interest: The authors declare no conflict of interest.

Appendix A. Fire-Growth Coefficients for Vehicle Fires

Table A1. Fire-Growth Coefficients for one and two vehicle fires.

Time	One Vehicle	Two Vehicles	Time	One Vehicle	Two Vehicles
55	0.000122845	0	111	-0.00003228	0
56	0.000110589	0	112	-0.000100544	0
57	0.000111826	0	113	-0.000102829	0
58	0.000119181	0	114	-0.000125789	0
59	0.000151472	0	115	-0.000112598	0
60	0.000143496	0	116	-0.000120963	0
61	0.000141763	0	117	-0.000118931	0
62	0.000142229	0	118	-0.000123675	0
63	0.00014096	0	119	-0.000136618	0
64	0.00013857	0	120	-0.000132197	0
65	0.000130619	0	121	-0.000123733	0
66	0.000143594	0	122	0.000045496	0
67	0.000153154	0	123	5.5872E-06	0
68	0.000143394	0	124	4.16544E-05	0
69	0.000115387	0	125	3059376E-05	0
70	0.000326219	0	126	3.63424E-05	0
71	0.000223675	0	127	3.67568E-05	0
72	0.000277621	0	128	2.67056E-05	0
73	0.000272314	0	129	-1.11936E-05	0
74	0.000274293	0	130	1.77728E-05	0
75	0.000288267	0	131	9.4848E-06	0
76	0.000282707	0	132	1.01104E-05	0
77	0.000298621	0	133	-3.34768E-05	0
78	0.000276741	0	134	0.00000116	0
79	0.000281992	0	135	0.000144683	0
80	0.000264557	0	136	0.000136411	0
81	0.000300158	0	137	0.000158899	0
82	0.000287592	0	138	0.000142838	0
83	0.000257986	0	139	0.000129723	0
84	0.000279203	0	140	0.000139946	0
85	0.000259619	0	141	0.000131667	0
86	0.000282691	0	142	0.000127328	0
87	0.000290432	0	143	0.000127696	0
88	0.000129774	0	144	0.000236862	0
89	0.000130891	0	145	0.000222347	0
90	0.000116182	0	146	0.000211238	0
91	0.000112029	0	147	0.000220477	0
92	0.000117714	0	148	0.000215518	0
93	0.000104933	0	149	0.00025139	0
94	0.00010421	0	150	0.00021375	0
95	0.000104573	0	151	0.000351069	0
96	0.000099011	0	152	0.000364856	0
97	0.0000978	0	153	0.000371894	0
98	0.00009746	0	154	0.00035011	0
99	0.0000985872	0	155	0.000354869	0
100	0.000088056	0	156	0.000278704	0
101	0.000102904	0	157	0.000365112	0
102	0.0000951808	0	158	0.00045428	0
103	0.000102624	0	159	0.00038917	0
104	-1.50448E-05	0	160	0.000341139	0
105	-9.12816E-05	0	161	0.000341352	0
106	-0.000100579	0	162	0.000358957	0
107	-9.69392E-05	0	163	0.000454278	0
108	-9.98464E-05	0	164	0.000407691	0
109	-2.65664E-05	0	165	0.000914008	0
110	-3.36192E-05	0	166	0.000862808	0

Table A1. Cont.

Time	One Vehicle	Two Vehicles	Time	One Vehicle	Two Vehicles
167	0.001054307	0.000220694	203	0.0100165	0.0120997
168	0.001063165	0.000611402	204	0.0110054	0.0114384
169	0.00104391	0.00068039	205	0.0110963	0.0124061
170	0.001228091	0.000880261	206	0.0101954	0.01114076
171	0.001635272	0.000812598	207	0.0104325	0.0122057
172	0.001834352	0.001029643	208	0.0106026	0.0121818
173	0.001916245	0.001240034	209	0.0111004	0.0124914
174	0.00199748	0.002309933	210	0.0111064	0.0135382
175	0.001945301	0.002533862	211	0.0126027	0.0129667
176	0.002285653	0.002699115	212	0.0107972	0.01428483
177	0.002352554	0.002952645	213	0.011416	0.0135615
178	0.002293226	0.002970237	214	0.0117953	0.0138855
179	0.003488533	0.003338856	215	0.0112167	0.0142959
180	0.003595838	0.003579187	216	0.0117955	0.0135957
181	0.003715666	0.00413451	217	0.0123651	0.0139167
182	0.004403666	0.0041032	218	0.011948	0.0153101
183	0.004578416	0.004038008	219	0.0121137	0.013121
184	0.00505969	0.005178826	220	0.0118276	0.0146671
185	0.004863582	0.006157565	221	0.0121345	0.0160241
186	0.005264023	0.007279477	222	0.0121715	0.0140538
187	0.005925605	0.007346544	223	0.0121353	0.0150714
188	0.005557421	0.006510378	224	0.0125515	0.0146725
189	0.006212605	0.007681355	225	0.0120098	0.0150361
190	0.006590218	0.007854469	226	0.0126213	0.0147933
191	0.005883032	0.007422917	227	0.0113123	0.0146584
192	0.003584963	0.007919211	228	0.0113451	0.0153618
193	0.0066938	0.0087581	229	0.0112896	0.0158492
194	0.0082796	0.0090616	230	0.0117224	0.0150186
195	0.008573	0.0095076	231	0.0121374	0.0151767
196	0.0081337	0.010333	232	0.0122526	0.0159671
197	0.0084333	0.0105719	233	0.0122324	0.0157199
198	0.0092459	0.0096946	234	0.0120766	0.0158552
199	0.0098028	0.0101741	235	0.0121153	0.0149351
200	0.0101057	0.0114833	236	0.0119933	0.0169582
201	0.009347	0.011416	237	0.0112681	0.0161582
202	0.0100612	0.0113177	238	0.0123996	0.016821

References

- Li, Y.; Spearpoint, M. Analysis of vehicle fire statistics in New Zealand parking buildings. *Fire Technol.* **2007**, *43*, 93–106. [\[CrossRef\]](#)
- Babrauskas, V. The Cone Calorimeter. In *SFPE Handbook of Fire Protection Engineering*; Springer: New York, NY, USA, 2016; pp. 952–980.
- Wang, Z.; Hu, X.; Jia, F.; Galea, E.R. A two-step method for predicting time to flashover in room corner test fires using cone calorimeter data. *Fire Mater.* **2012**, *37*, 457–473. [\[CrossRef\]](#)
- Lai, C.M.; Ho, M.C.; Lin, T.H. Experimental Investigations of Fire Spread and Flashover Time in Office Fires. *J. Fire Sci.* **2010**, *28*, 279–302. [\[CrossRef\]](#)
- Hakkarainen, T. Rate of Heat Release and Ignitability Indices in Predicting SBI Test Results. *J. Fire Sci.* **2001**, *19*, 284–305. [\[CrossRef\]](#)
- Katsuhiko, O.; Norimichi, W.; Yasuaki, H.; Tadaomi, C.; Ryoji, M.; Hitoshi, M.; Satoshi, O.; Hideki, S.; Yohsuke, T.; Kimio, H.; et al. Burning behavior of sedan passenger cars. *Fire Saf. J.* **2009**, *44*, 301–310. [\[CrossRef\]](#)
- Mangs, J.; Keski-Rahkonen, O. Characterization of the Fire Behaviour of a Burning Passenger Car. Part1: Car Fire Experiments. *Fire Saf. J.* **1994**, *23*, 17–35. [\[CrossRef\]](#)

8. Katsuhiko, O.; Takuma, O.; Hiroki, M.; Masakatsu, H.; Norimichi, W. Burning behavior of minivan passenger cars. *Fire Saf. J.* **2013**, *62*, 272–280. [[CrossRef](#)]
9. Li, D.; Zhu, G.; Zhu, H.; Yu, Z.; Gao, Y.; Jiang, X. Flame spread and smoke temperature of full-scale fire test of car fire. *Case Stud. Therm. Eng.* **2017**, *10*, 315–324. [[CrossRef](#)]
10. Loladze, I. Rising atmospheric CO₂ and human nutrition: Toward globally imbalanced plant stoichiometry? *Trends Ecol. Evol.* **2002**, *17*, 457–461. [[CrossRef](#)]
11. Bailey, J.E.; Argyropoulos, S.V.; Kendrick, A.H.; Nutt, D.J. Behavior and Cardiovascular Effects of 7.5% CO₂ in Human Volunteers. *Med. J. Aust.* **2005**, *21*, 18–25. [[CrossRef](#)]
12. Mayr, F.B.; Spiel, A.; Leitner, J.; Marsik, C.; Germann, P.; Ullrich, R.; Wagner, O.; Jilma, B. Effects of Carbon Monoxide inhalation during Experimental Endotoxemia in Humans. *Am. J. Respir. Crit. Care Med.* **2005**, *171*, 354–360. [[CrossRef](#)] [[PubMed](#)]
13. Truchot, B.; Fouillen, F.; Collet, S. An experimental evaluation of toxic gas emissions from vehicle fires. *Fire Saf. J.* **2018**, *97*, 111–118. [[CrossRef](#)]
14. Deckers, X.; Haga, S.; Sette, B.; Merci, B. Smoke control in case of fire in a large car park: Full-scale experiments. *Fire Saf. J.* **2013**, *57*, 11–21. [[CrossRef](#)]
15. Yan, Z.; Guo, Q.; Zhu, H. Full-scale experiments on fire characteristics of road tunnel at high altitude. *Tunn. Undergr. Space Technol.* **2017**, *66*, 134–146. [[CrossRef](#)]
16. Blanchard, E.; Boulet, P.; Desanghere, S.; Cesmat, E.; Meyrand, R.; Garo, J.P.; Vantelon, J.P. Experimental and numerical study of fire in a midscale test tunnel. *Fire Saf. J.* **2012**, *47*, 18–31. [[CrossRef](#)]
17. Lonnermark, A.; Ingason, H. Fire Spread and Flame Length in Large-Scale Tunnel Fires. *Fire Technol. J.* **2006**, *42*, 283–302. [[CrossRef](#)]
18. Horvath, I.; Beeck, J.V.; Merci, B. Full-scale and reduced-scale tests on smoke movement in case of car park fire. *Fire Saf. J.* **2013**, *57*, 35–43. [[CrossRef](#)]
19. Ingason, H. Model scale railcar fire tests. *Fire Saf. J.* **2007**, *42*, 271–282. [[CrossRef](#)]
20. Lee, S.R.; Ryou, H.S. An experimental study of the effect of the aspect ratio on the critical velocity in longitudinal ventilation tunnel fires. *Fire Sci. J.* **2005**, *23*, 119–138. [[CrossRef](#)]
21. Lee, S.R.; Ryou, H.S. A numerical study on smoke movement in longitudinal ventilation tunnel fires for different aspect ratio. *Build. Environ. J.* **2006**, *41*, 719–725. [[CrossRef](#)]
22. Baek, D.; Bae, S.; Ryou, H.S. A numerical study on the effect of the hydraulic diameter of tunnels on the plug-holing phenomena in shallow underground tunnels. *J. Mech. Sci. Technol.* **2017**, *31*, 2331–2338. [[CrossRef](#)]
23. Baek, D.; Sung, K.H.; Ryou, H.S. Experimental study on the effect of heat release rate and aspect ratio of tunnel on the plug-holing phenomena in shallow underground tunnels. *Int. J. Heat Mass Transf.* **2017**, *113*, 1135–1141. [[CrossRef](#)]
24. McCaffrey, B. Flame Height. In *SFPE Handbook of Fire Protection Engineering*, 2nd ed.; National Fire Protection Assoc.: Quincy, MA, USA, 1995.
25. Heskestad, G. Fire Plumes. In *SFPE Handbook of Fire Protection Engineering*, 2nd ed.; National Fire Protection Assoc.: Quincy, MA, USA, 1995.
26. Melcher, T.; Zonke, R.; Trott, M.; Krause, U. Experimental investigations on the repeatability of real scale fire test. *Fire Saf. J.* **2016**, *82*, 101–114. [[CrossRef](#)]
27. Park, Y.; Lee, Y.; Na, J.; Ryou, H.S. Numerical Study on the Effect of Tunnel Aspect Ratio on Evacuation with Unsteady Heat Release Rate Due to Fire in the Case of Two Vehicles. *Energies* **2019**, *12*, 133. [[CrossRef](#)]
28. Shipp, M.; Spearpoint, M. Measurements of the severity of fires involving private motor vehicles. *Fire Mater.* **1995**, *19*, 143–151. [[CrossRef](#)]
29. Ingason, H. *An Overview of Vehicle Fires in Tunnels*; SP Swedish National Testing and Research Institute: Boras, Sweden, 2001.
30. Agency for Toxic Substances and Disease Registry (ATSDR). Available online: www.atsdr.cdc.gov/2012 (accessed on 27 February 2019).

